



## **Numerical methods for accelerator beam probe calibration**

Stanley Humphries, Ph.D.

**Field Precision LLC**  
E mail: [techinfo@fieldp.com](mailto:techinfo@fieldp.com)  
Internet: <https://www.fieldp.com>

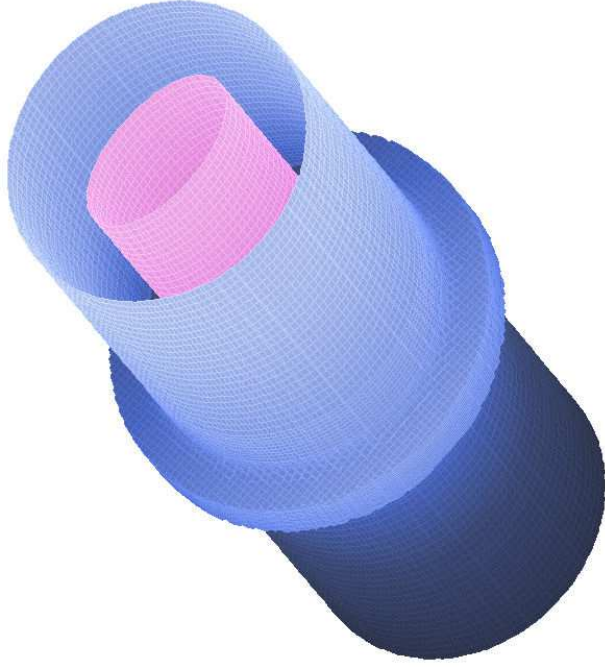


Figure 1: View of the calculation geometry. Center conductor in red. Inner boundary of outer wall in blue.

This tutorial describes three-dimensional calculations of magnetic field distributions in the  $dB/dt$  probe calibration test stand for the DARHT II accelerator at Los Alamos National Laboratory. Center conductors with elliptical cross sections have been employed to study the feasibility of non-interceptive probe arrays to measure cross sections of non-circular electron beams. Figure 1 shows the simulation geometry with the center conductor displayed in red. Table 1 lists the major and minor radii of the five elliptical center-conductor inserts. The inside boundary of the chamber wall is displayed in blue in Fig. 1. The circular tube has an inner radius 2.905". The probe array is located in a slot with outer radius 3.685" and length 1.000". Eight  $dB/dt$  probes at intervals of  $45^\circ$  are oriented to sense the azimuthal component of magnetic field. Each probe has an effective inner radius  $R_i = 2.905''$ , outer radius  $R_o = 3.612''$  and length  $L = 0.707''$ . The probe area is  $3.225 \times 10^{-4} \text{ m}^2$ .

The simulations were performed with **Magnum**, a three dimensional finite-element program employing a mesh of conformal hexahedron elements. The program can model ideal conducting boundaries. As a result, the calculated fields include effects of self-consistent distributions of drive current on the center conductor and return current on the wall. Two input files are required for each run:

Table 1: Center-conductor dimensions

Run	$R_x$ (inch)	$R_x$ (inch)
01	1.246	1.246
02	1.310	1.190
03	1.370	1.140
04	1.480	1.055
05	1.675	0.930

BDOT.CDF: definition of drive currents.

BDOTOX.MIN: computational mesh with magnetically-active elements.

For this calculation, the drive current was a single filament of effectively infinite length (80.0”) carrying 1.0 A along the the  $z$  axis. The **MetaMesh** input file BDOT05.MIN is shown in Appendix 1. The variable resolution mesh gave good numerical accuracy near the probe slot. The air region ( $\mu_r = 1.0$ ) was a turning that carved out the shaped inner boundary of the outer wall. The turning boundary was defined by a connected set of line and arc vectors. Figure 2 shows a two-dimensional view of the completed mesh. The inner and outer conductors were antiferromagnetic materials with  $\mu_r = 10^{-4}$ . Magnum has the useful property that it generates the correct distribution of surface current on the inner conductor, independent of the shape and position of the enclosed drive current. The Magnum control script is listed in Table 2. Figure 3 shows the calculated field in the plane  $z = 0.0$ ” for run BDOT05.

A circular conductor was used for the initial run (BDOT01). Field scans were performed over the radial span of the probe area at axial locations  $z = 0.00$ ” and  $z = \pm 0.340$ ”. As expected, the field was purely azimuthal. The values were independent of axial position (to within  $\pm 0.1\%$ ) and followed the radial variation  $r^{-1}$  to within 0.3%. The azimuthally averaged value at radius 3.246” was  $2.410 \pm 0.0056$   $\mu$ tesla, compared to the theoretical prediction of 2.426  $\mu$ tesla. The same calculations were performed with a highly elliptical center conductor (BDOT05) along lines at  $\theta = 45^\circ$ . Figure 4 plots the magnitude of the field as a function of radius at the slot center ( $z = 0.0$ ”) and edge ( $z = 0.340$ ”). The values are indistinguishable. The field components  $-B_x$  and  $B_y$  are plotted in Fig. 5 as a function of radius at the slot center. Because of the shaped center conductor, the field was not normal to the radial line at the entrance to the slot, but rather had an inclination angle of  $138.8^\circ$ . A similar result was observed in a scan at  $z = 0.340$ ”. The effect of the angular error on the magnetic flux would be quite small,  $\cos(3.8^\circ) = 0.998$ .

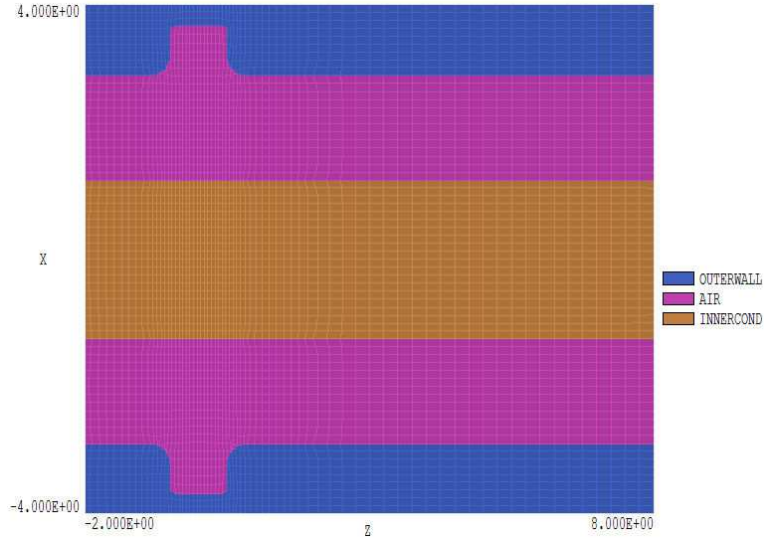


Figure 2: Conformal mesh for run BDOT01, section in the plane  $y = 0.0$ .

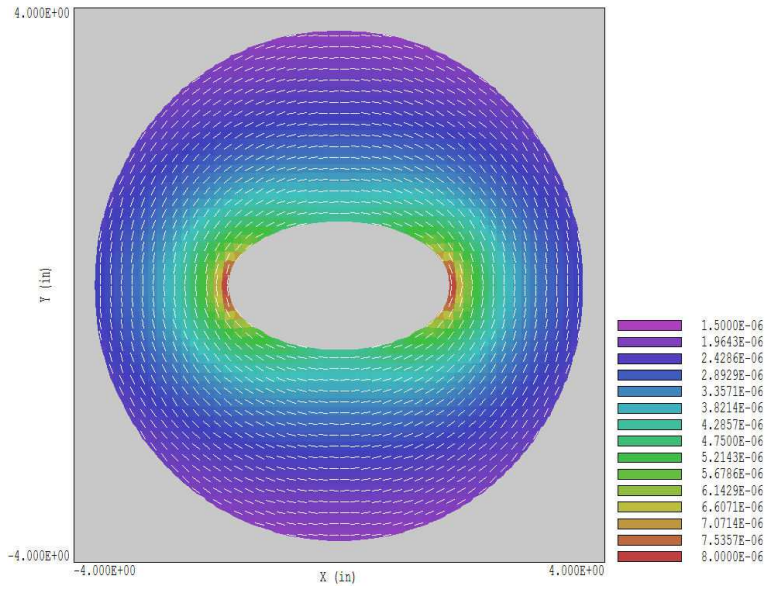


Figure 3: Field calculation in the plane  $z = 0.0$  for run BDOT05. The plot shows vectors parallel to the magnetic field lines and color-coding by  $|\mathbf{B}|$ .

Table 2: File BDOT05.GIN

```
* MagNum 2.0 Script (Field Precision)
* File: BDOT05.GIN
* Date: 01/19/2007
* Time: 09:46:34
SolType = STANDARD
Mesh = BDOT05
Source = BDOT
DUnit = 3.9370E+01
ResTarget = 1.0000E-08
MaxCycle = 1000
* Region 1: OUTERWALL
Mu(1) = 1.0000E-04
* Region 2: AIR
Mu(2) = 1.0000E+00
* Region 3: INNERCOND
Mu(3) = 1.0000E-04
EndFile
```

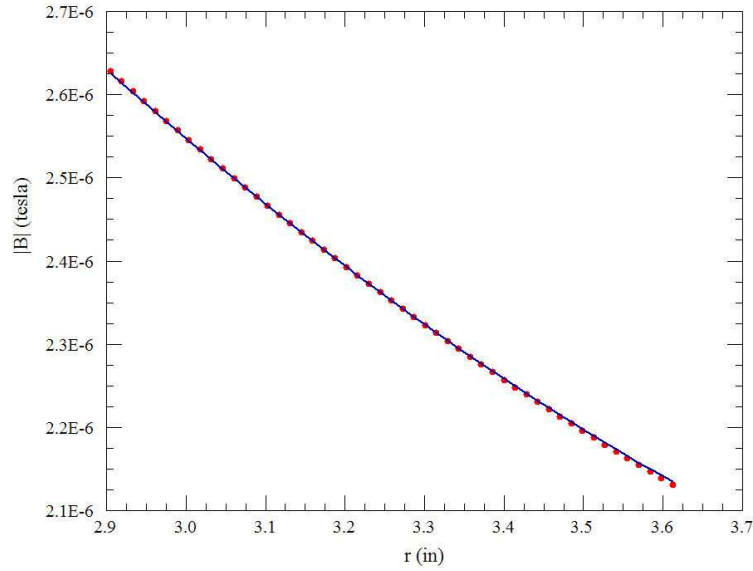


Figure 4: Plot of  $|\mathbf{B}|$  as a function of  $r$  along a  $45^\circ$  line for a highly elliptical center conductor (BDOT05). Solid line:  $z = 0.000''$ . Symbols:  $z = 0.340''$ .

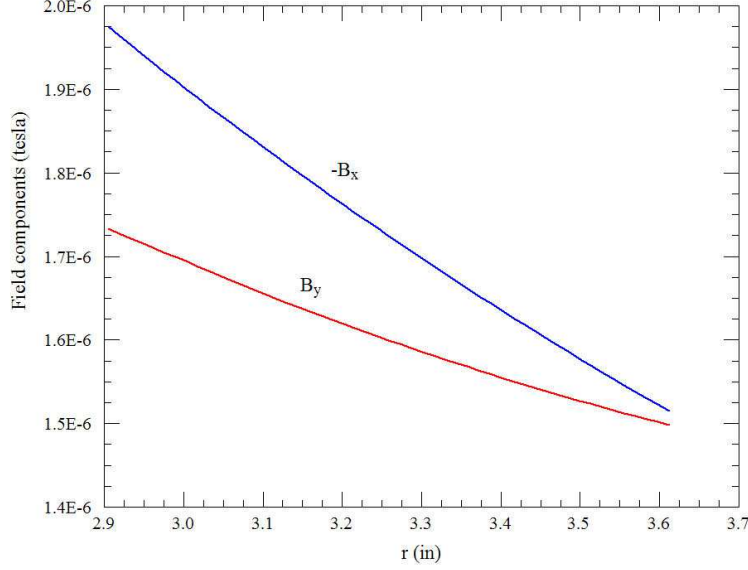


Figure 5: Plot of  $-B_x$  and  $B_y$  as a function of radial position in the probe loop along a  $45^\circ$  line at  $z = 0.000''$  for a highly elliptical center conductor (BDOT05).

Following the above results, we can make a good estimate of the magnetic flux enclosed by the probes by taking an average of the field magnitude over radius and multiplying by the probe area. We have seen that the magnetic field closely follows the variation  $B_\theta = A/r$ . Therefore, the radial average over the probe is

$$\overline{B_\theta} = A \frac{\ln(R_o/R_i)}{R_o - R_i}. \quad (1)$$

The field equals the average value at radius  $\overline{R}$  where  $B_\theta = A/\overline{R}$ . A comparison to Eq. 1 gives

$$\overline{R} = \frac{R_o - R_i}{\ln(R_o/R_i)}. \quad (2)$$

Inserting the probe dimensions, we find that  $\overline{R} = 3.246''$ .

The main task of the study was the calculation of  $|\mathbf{B}|$  at  $r = 3.246''$  and  $z = 0.000''$  as a function of azimuth in the range  $0.0^\circ \leq \theta \leq 90.0^\circ$  for the five geometries listed in Table 1. The results are plotted in Fig. 6. The curve for run BDOT01 gives a sense of the numerical accuracy. In theory, the values should be identical but vary because of small differences in interpolations relative to the conformal mesh. Table 3 contains the numerical data used to generate the plot.

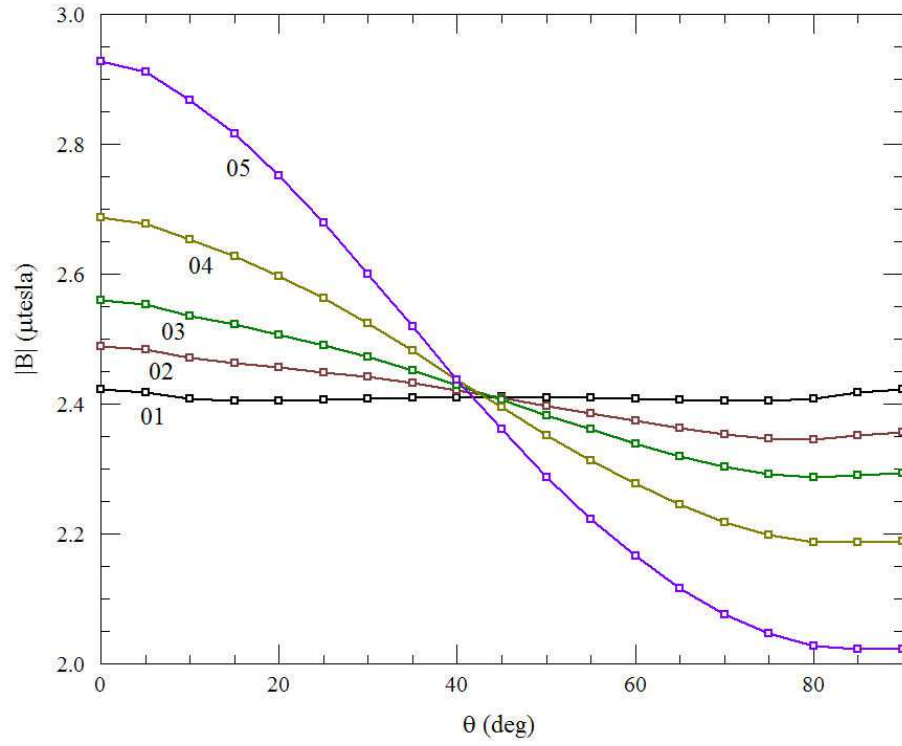


Figure 6: Plot of  $|\mathbf{B}|$  at  $r = 3.246''$  and  $z = 0.000''$  as a function of  $\theta$  for the five center-conductor geometries.

Table 3: Magnetic flux-density magnitude (in  $\mu$ tesla) as a function of  $\theta$  at  $r = 3.246''$ ,  $z = 0.00$

Angle	BDOT01	BDOT02	BDOT03	BDOT04	BDOT05
0.0	2.4219	2.4892	2.5599	2.6878	2.9275
5.0	2.4173	2.4835	2.5528	2.6778	2.9110
10.0	2.4078	2.4707	2.5360	2.6531	2.8684
15.0	2.4045	2.4625	2.5218	2.6271	2.8159
20.0	2.4043	2.4557	2.5072	2.5970	2.7522
25.0	2.4057	2.4487	2.4907	2.5621	2.6787
30.0	2.4082	2.4416	2.4728	2.5240	2.6006
35.0	2.4099	2.4325	2.4523	2.4825	2.5195
40.0	2.4095	2.4207	2.4286	2.4378	2.4375
45.0	2.4110	2.4104	2.4065	2.3953	2.3609
50.0	2.4096	2.3972	2.3820	2.3519	2.2876
55.0	2.4099	2.3862	2.3605	2.3132	2.2231
60.0	2.4078	2.3739	2.3388	2.2767	2.1655
65.0	2.4057	2.3625	2.3194	2.2444	2.1160
70.0	2.4041	2.3531	2.3031	2.2178	2.0757
75.0	2.4043	2.3470	2.2918	2.1984	2.0461
80.0	2.4076	2.3457	2.2866	2.1873	2.0277
85.0	2.4172	2.3523	2.2906	2.1874	2.0229
90.0	2.4219	2.3558	2.2931	2.1885	2.0223



## Appendix 1. File BDOT05.MIN

```

* Elliptical axes: 1.675  0.930
GLOBAL
  XMesh
    -4.000  4.000  0.125
  End
  YMesh
    -4.000  4.000  0.125
  End
  ZMesh
    -8.000 -2.000  0.250
    -2.000 -0.850  0.125
    -0.850  0.850  0.0625
    0.850  2.000  0.125
    2.000  8.000  0.250
  End
  RegName(1): OuterWall
  RegName(2): Air
  RegName(3): InnerCond
END
PART
  Region: OuterWall
  Type: Box
  Fab: 8.000 8.000 20.000
END
PART
  Region: Air
  Type: Turning
  L -11.000 2.905 -0.810 2.905 S
  A -0.810 2.905 -0.500 3.215 -0.810 3.215 S
  L -0.500 3.215 -0.500 3.685 S
  L -0.500 3.685 0.500 3.685 S
  L 0.500 3.685 0.500 3.215 S
  A 0.500 3.215 0.810 2.905 0.810 3.215 S
  L 0.810 2.905 11.000 2.905 S
  L 11.000 2.905 11.000 0.000
  L 11.000 0.000 -11.000 0.000
  L -11.000 0.000 -11.000 2.905
  End
  Surface Region OuterWall
  Coat OuterWall OuterWall
END
PART
  Region: InnerCond
  Type: EllipCyl
  Fab: 1.675 0.930 22.00
  Surface Region Air
END
ENDFILE

```